NASA TECHNICAL MEMORANDUM

NASA TM X- 72000

COPY NO.

NASA TM X- 72000

A SIMPLE METHOD OF CALCULATING POWER-LAW VELOCITY PROFILE EXPONENTS FROM EXPERIMENTAL DATA

BY JERRY M. ALLEN

LANGLEY RESEARCH CENTER
LANGLEY STATION, HAMPTON, VA.

NATIONAL AERONAUTICS AND SPACE ADMINISTRATION
LANGLEY RESEARCH CENTER, HAMPTON, VIRGINIA 23665

1. Report No.	2. Government Accession No.	3. Recipient's Catalog No.
TMX 72000		

4. Title and Subtitle	5. Report Date
A Simple Method of Calculating Power-Law Velocity Profile Exponents From Experimental Data	October 1974
	6. Performing Organization Code
7. Author(s)	8. Performing Organization Report No.
Jerry M. Allen	
9. Performing Organization Name and Address	10. Work Unit No.
NASA Langley Research Center Hampton, Virginia 23665	505-11-15-02
	11. Contract or Grant No.
	13. Type of Report and Period Covered
12. Sponsoring Agency Name and Address	Technical Memorandum
National Aeronautics and Administration Washington, DC 20546	14. Sponsoring Agency Code

15. Supplementary Notes

16. Abstract

Analytical expressions for the effects of compressibility and heat transfer on laminar and turbulent shape factors H have been developed. Solving the turbulent equation for the power law velocity profile exponent N has resulted in a simple technique by which the N values of experimental turbulent profiles can be calculated directly from the integral parameters. Thus the data plotting, curve fitting, and slope measuring, which is the normal technique of obtaining experimental N values, is eliminated. The N values obtained by this method should be within the accuracy with which they could be measured.

17. Key Words (Suggested by Author(s)) (STAR category underlined)	18. Distribution Statement
Boundary Layer Power Law Shape Factor	Unclassified-Unlimied Star Category 12

19. Security Classif. (of this report)	20. Security Classif. (of this page)	21. No. of Pages	22. Price*
Unclassified	Unclassified	22	$3.00

*Available from { The National Technical Information Service, Springfield, Virginia 22151
STIF/NASA Scientific and Technical Information Facility, P.O. Box 33, College Park, MD 20740

A SIMPLE METHOD OF CALCULATING POWER-LAW VELOCITY PROFILE EXPONENTS FROM EXPERIMENTAL DATA

By Jerry M. Allen
Langley Research Center

SUMMARY

Analytical expressions for the effects of compressibility and heat transfer on laminar and turbulent shape factors H have been developed. Solving the turbulent equation for the power law velocity profile exponent N has resulted in a simple technique by which the N values of experimental turbulent profiles can be calculated directly from the integral parameters. Thus the data plotting, curve fitting, and slope measuring, which is the normal technique of obtaining experimental N values, is eliminated. The N values obtained by this method should be within the accuracy with which they could be measured.

INTRODUCTION

It has long been known that turbulent velocity profiles may be represented by a power law of the form

$$\frac{u}{u_e} = \left(\frac{y}{\delta}\right)^{\frac{1}{N}} \tag{1}$$

where N generally varies from about 5 to 11 for turbulent velocity profiles. Figure 1(a) shows one-fifth and one-eleventh power law profiles plotted in the conventional manner.

Since the exponent N represents the general shape of the profile, the experimenter often obtains N values of his profiles as a useful index of profile shape. The usual method of obtaining these experimental N values is to plot the velocity profile in logarithmic form, fit a straight line through the data, and measure the slope of this line. Figure 1(b) shows how these one-fifth and one-eleventh power law profiles

appear in logarithmic form. This process is rather tedious and time consuming, especially when a large number of profiles is involved.

It is a common practice in the conduct of boundary layer experiments to obtain from the measured profiles certain integral parameters, such as displacement thickness δ^* and momentum thickness θ , which are descriptive of the character of the flow. These parameters are obtained by a process which is independent of the method normally used to define the profile N values.

The objectives of this paper are to develop an analytical expression for the effects of compressibility and heat transfer on the turbulent shape factor, to compare this expression with a similar one for the laminar shape factor, and to demonstrate how this turbulent expression may be used as a simple method of calculating the N values of experimental turbulent velocity profiles, thus eliminating the need of logarithmic data plotting, curve fitting, and slope measuring.

NOMENCLATURE

H	shape factor, δ^*/θ
M	Mach number
N	power law velocity profile exponent, $\frac{u}{u_e} = \left(\frac{y}{\delta}\right)^{\frac{1}{N}}$
R_θ	Reynolds number based on momentum thickness
T	temperature
u	velocity in streamwise direction
y	normal coordinate
γ	ratio of specific heats (= 1.4 for air)
δ	boundary layer total thickness
δ^*	boundary layer displacement thickness
θ	boundary layer momentum thickness

ρ	density
σ	Prandtl number (0.72 for air)

Subscripts:

aw	adiabatic wall
c	calculated
e	boundary layer edge
i	incompressible
m	measured
t	tabulated
w	wall

DEVELOPMENT OF TURBULENT SHAPE FACTOR EQUATION

In incompressible flow the ratio of displacement thickness δ^*_i to momentum thickness θ_i is strictly a function of the shape of the velocity profile and is, indeed, called the shape factor. Hence it is possible to relate δ^*_i and θ_i to N, as described below.

The incompressible-flow forms of the displacement and momentum thicknesses are

$$\left.\begin{aligned} \delta^*_i &\equiv \int_0^\delta \left(1 - \frac{u}{u_e}\right) dy \\ \text{and} \quad \theta_i &\equiv \int_0^\delta \frac{u}{u_e}\left(1 - \frac{u}{u_e}\right) dy \end{aligned}\right\} \qquad (2)$$

Assuming a power law velocity profile in the form of equation (1) permits the closed-form integration of equations (2). Thus

$$\delta^*_i = \frac{\delta}{N + 1} \tag{3}$$

and

$$\theta_i = \frac{N\,\delta}{(N + 1)\,(N + 2)} \tag{4}$$

Dividing equation (3) by equation (4) yields the incompressible shape factor

$$H_i = \frac{N + 2}{N} \tag{5}$$

In compressible flow the situation is not so straightforward since the displacement and momentum thicknesses

$$\left.\begin{aligned} \delta^* &= \int_0^{\delta} \left(1 - \frac{\rho u}{\rho_e u_e}\right) dy \\ \text{and} \quad \theta &= \int_0^{\delta} \frac{\rho u}{\rho_e u_e} \left(1 - \frac{u}{u_e}\right) dy \end{aligned}\right\} \tag{6}$$

are no longer strictly functions of the velocity profile shape. The compressibility effects contained in the density profile result in integrals which do not have general closed-form solutions. The functional relationship of equations (6) may be expressed as $H = H\left(N, M_e, \frac{T_w - T_{aw}}{T_e}\right)$.

For the zero heat transfer case ($T_w = T_{aw}$) H reduces to $H_{aw} = H_{aw}(N, M_e)$. Reference 1 has numerically integrated equations (6) for this zero heat transfer case, and has tabulated H_{aw} as a function of N and M_e. This function would be much more useful if it could be put in analytic rather than tabular form. Hence, an attempt was made in this study to analytically define the functional relationship $H_{aw} = H_{aw}(N, M_e)$, as described below.

Figure 2 was prepared from the tables of reference 1 to show the variation of H_{aw} with N and M_e. If H_{aw} is viewed as being composed of H_i (N) plus a compressibility correction term ΔH (N, M_e), we can write

$$H_{aw} = H_i\ (N) + \Delta H\ (N, M_e) \tag{7}$$

The variation of H_{aw} with M_e appears exponential. Hence if we assume that $H \equiv H_{aw} - H_i = f(N)\, M_e^{x}$, the exponent x can be obtained from the slope of the logarithmic plot of H_{aw} and M_e; that is

$$x = -\frac{\partial \log_e(\Delta H)}{\partial \log_e(M_e)}$$

Figure 3 shows that the exponential variation fits the data very well, and that the value of the exponent is about 1.989 .

$$\text{Hence } \Delta H = f(N)\, M_e^{1.989} \qquad (8)$$

$$\text{or} \quad \frac{\Delta H}{M_e^{1.989}} = f(N)$$

Figure 4 shows how the parameter $\frac{\Delta H}{M_e^{1.989}}$ varies with N. The function f(N) was estimated from this figure to be

$$f(N) = 0.4099 + \frac{0.2719}{N} \qquad (9)$$

Hence the desired relationship between H, N, and M_e for turbulent adaiabatic flow is obtained by inserting equations (5), (8), and (9) into equation (7) . Thus

$$H_{aw} = 1.0 + \frac{2.0}{N} + \left(0.4099 + \frac{0.2719}{N}\right) M_e^{1.989} \qquad (10)$$

For given values of N and M_e, comparisons were made between the values of H_{aw} calculated by equation (10) and Tucker's tabulated values. For the range $5 \le N \le 11$ and $0 \le M_e \le 5$, which is the range on which equation (10) was derived, the disagreement between calculated and tabulated H_{aw} values is less than 0.3 percent. Even up to $M_e = 10$, which is the limit of the tabulated data, the disagreement is less than 0.5 percent. Thus equation (10) provides a satisfactory approximation for the turbulent adiabatic shape factor as expressed in Tucker's table.

Persh and Lee (reference 2) have numerically integrated equations (6) for the heat transfer case, and have tabulated H as a function of N, M_e , and $\frac{T_w - T_{aw}}{T_e}$. In order to get an analytical expression for this

general case, H was viewed in this paper as being composed of the zero heat transfer value H_{aw} plus a correction term due to heat transfer $\overline{\Delta H}$. Thus we may write

$$H\left(N, M_e, \frac{T_w - T_{aw}}{T_e}\right) = H_{aw}\,(N, M_e, 0) + \overline{\Delta H}\left(N, M_e, \frac{T_w - T_{aw}}{T_e}\right) \qquad (11)$$

Figure 5 was prepared from the tables of reference 2 to show the variation of $\overline{\Delta H}$ $(\equiv H - H_{aw})$ with the heat transfer parameter $\frac{T_w - T_{aw}}{T_e}$ for Mach numbers of 0 and 5, and N values of 5 and 11 . This variation is approximately linear. Hence we may write

$$\overline{\Delta H} = g(N, M_e)\ \frac{T_w - T_{aw}}{T_e} \qquad (12)$$

Moreover, Mach number has a very small effect on the function g, as shown in Table I where the g values were measured from figure 5 .

TABLE I - MEASURED VALUES OF g

N	M_e	g	
5	0	1.286	1.27
5	5	1.256	
11	0	1.143	1.13
11	5	1.124	

If the dependency of g on M_e is eliminated, eq. (12) can be written

$$\overline{\Delta H} = g(N)\ \frac{T_w - T_{aw}}{T_e} \qquad (13)$$

Assuming a linear variation of g with N, the following equation can be derived from Table I .

$$g(N) = 1.39 - 0.024N \qquad (14)$$

Hence equation (13) becomes

$$\overline{\Delta H} = (1.39 - 0.024N)\ \frac{T_w - T_{aw}}{T_e} \qquad (15)$$

Comparisons were made between the values of $\overline{\Delta H}$ calculated from equation (15) and those taken from the tables of reference 2 . The disagreement between the calculated and tabulated values over the range of variables

covered by the tables ($0 \le M_e \le 20$, $5 \le N \le 11$, and $-10 \le \frac{T_w - T_{aw}}{T_e} \le 10$) was less than ± 2 percent .

Hence the general expression for the turbulent shape factor as a function of power-law exponent, Mach number, and heat transfer can be obtained by inserting equations (10) and (15) into equation (11) .

$$H = 1.0 + \frac{2.0}{N} + \left(0.4099 + \frac{0.2719}{N}\right) M_e^{1.989} + (1.39 - 0.024N) \frac{T_w - T_{aw}}{T_e} \qquad (16)$$

COMPARISON OF LAMINAR AND TURBULENT SHAPE FACTOR EQUATIONS

An approximate relation for the effect of compressibility on laminar shape factor has been derived by Monaghan in reference 3. The relation is

$$H = \frac{2\pi A - \pi D - 4B - 4}{4 - \pi} \qquad (17)$$

where

$$A = \frac{T_w}{T_e}$$

$$B = \sqrt[3]{\sigma}\left(\frac{T_w}{T_e} - \frac{T_{aw}}{T_e}\right)$$

$$D = \sigma\left(\frac{\gamma - 1}{2}\right) M_e^2$$

Hence equation (17) becomes

$$H = \frac{2\pi \frac{T_{aw}}{T_e} - \pi\sigma\left(\frac{\gamma - 1}{2}\right) M_e^2 - 4 + \left(2\pi - 4\sqrt[3]{\sigma}\right) \frac{T_w - T_{aw}}{T_e}}{4 - \pi} \qquad (18)$$

The adiabatic wall temperature ratio in laminar flow is

$$\frac{T_{aw}}{T_e} = 1 + \frac{\gamma - 1}{2} \sqrt{\sigma}\, M_e^2 \qquad (19)$$

Inserting equation (19) into equation (18) results in the following expression for $\gamma = 1.4$ and $\sigma = 0.72$.

$$H = 2.660 + 0.715\ M_e^2 + 3.143\ \left(\frac{T_w - T_{aw}}{T_e}\right) \qquad (20)$$

Figure 6 shows comparisons between the laminar and turbulent shape factors, equation (20) and (16) , respectively. The general trends are similar; however, both Mach number and wall temperature have somewhat larger effects on the laminar shape factor. For experimental data in which the integral parameters δ^* and θ are known, figure 6 can be used as a convenient criterion to determine if a profile is laminar or turbulent.

CALCULATION OF POWER-LAW EXPONENT FROM SHAPE FACTOR

Note that the adiabatic turbulent shape factor equation developed in this paper - equation (10) - may be easily solved for the power law exponent N.

$$N = \frac{2.0 + 0.2719\ M_e^{1.989}}{H_{aw} - 1.0 - 0.4099\ M_e^{1.989}} \qquad (21)$$

Thus it should be possible for a given freestream Mach number to calculate the N values of turbulent profiles directly from experimental integral parameters.

If the incompressible turbulent shape factor equation (equation (5)) is solved for N, the result is

$$N = \frac{2}{H_i - 1} \qquad (22)$$

Note that for the case of $M_e = 0$, equation (21) reduces to equation (22) .

The calculation of N by this technique can be accomplished by one of the following methods: (1) For profiles in which $T_w \approx T_{aw}$, N can be calculated directly from H_{aw} and M_e by equation (21); or (2) For profiles obtained under heat transfer conditions, N can be interpolated from equation (16) from known values of H, M_e , and $\frac{T_w - T_{aw}}{T_e}$; or (3) For any profile in which the incompressible, or kinematic, forms of displacement and momentum

thicknesses are known, N can be calculated from H_i by equation (22) . Note that this third method is not restricted to $M_e = 0$ or $T_w = T_{aw}$ profiles even though H_i is used in the calculations .

Since integration of experimental data to obtain δ^* and θ is a normal data reduction procedure, it would be a simple matter to integrate the same profiles to obtain δ^*_i and θ_i . Hence by using the appropriate method the experimenter can calculate the N values of his turbulent profiles without the need of data plotting, curve fitting and slope measuring.

EXAMPLES OF USE

Let us now examine a few adiabatic velocity profiles to see how the N values calculated by this technique (N_C and $N_{C,i}$) compare with measured values (N_m) . Reference 4 contains 12 turbulent velocity profiles at Mach numbers of 1.975, 2.320, and 4.630 . Table II lists the test conditions of these profiles, the integral parameters including N_C and $N_{C,i}$, and N_m measured in the conventional manner.

TABLE II - REFERENCE 4 DATA

PROFILE	M_e	R_θ	H_{aw}	H_i	N_c	$N_{c,i}$	N_m
1	1.975	3.62×10^4	3.002	1.275	7.35	7.27	7.41
2	2.320	1.48×10^4	3.594	1.238	8.46	8.43	8.50
3	2.320	2.38×10^4	3.575	1.228	8.88	8.78	8.63
4	2.320	4.42×10^4	3.554	1.217	9.37	9.21	9.06
5	2.320	6.41×10^4	3.534	1.207	9.91	9.63	9.45
6	2.320	8.04×10^4	3.532	1.204	9.98	9.83	9.24
7	4.630	1.07×10^4	10.508	1.237	8.91	8.44	9.00
8	4.630	1.69×10^4	10.490	1.233	9.10	8.58	9.20
9	4.630	3.11×10^4	10.418	1.214	9.94	9.37	10.20
10	4.630	4.44×10^4	10.369	1.200	10.60	9.98	10.83
11	4.630	5.71×10^4	10.343	1.194	11.00	10.31	11.11
12	4.630	6.81×10^4	10.322	1.188	11.33	10.66	11.31

A comparison of the experimental H values of this table with the curves of figure 6(a) reveals that these profiles are indeed turbulent. The ratios of calculated-to-measured N values are plotted in figure 7 to show that both N_C and $N_{C,\,i}$ are generally in good agreement with the measured values of N. Reference 5 has examined a large number of profiles and has estimated that N can be measured within an accuracy of about ±10 percent. For all the data presented in figure 7, the agreement between calculated and measured N values is within this accuracy. Also, note from Table II that at each Mach number both the calculated and measured N values show the expected trend of increasing N with increasing Reynolds number.

One of the profiles from reference 4 is examined in more detail in figure 8 . Straight lines were fitted to the outer part of the profile only (solid line) and the inner part only (dotted line) to illustrate the range of curve fits which could be drawn through this profile. The N values of these lines are 6.69 and 8.68 , respectively; which represent a ±13 percent range. Since it is unlikely that these extreme fits to the data would be performed, especially the inner profile fit, the range of N curves which would normally be fitted to this profile is probably close to the ±10 percent mentioned earlier . A more reasonable fit to the complete profile is represented by the dashed line, whose N value is 7.41 , which is very close to the calculated values for this profile (N_C = 7.35 and $N_{C,\,i}$ = 7.27).

Since this technique calculates N from either H, H_{aw}, or H_i , which are obtained by integration of the entire profile, the N values thus obtained represent a fit to the entire profile. Good results would not be obtained, therefore, for turbulent profiles containing a large laminar sublayer. Measurements in a laminar sublayer tend to reduce the calculated N values, with the extreme example being a completely laminar profile. For example, the integration of a Blasius profile yields $N_{C,\,i}$ = 1.26 . Since N ranges from about 5 to 11 for turbulent profiles, this technique could also be used as convenient criterion for determining whether a profile is laminar or turbulent.

One cautionary note about this technique needs mentioning. It can be determined from equation (21) that N is rather sensitive to errors in H. For example, integration errors which result in a one percent error in H

produce about a 10 percent error in N . Therefore in order to use this technique, accurate integration of experimental data is required.

CONCLUDING REMARKS

In summary, analytical expressions for the effects of compressibility and heat transfer on laminar and turbulent shape factors H have been developed. Solving the turbulent equation for the power law velocity profile exponent N has resulted in a simple technique by which the N values of experimental turbulent profiles can be caulculated directly from the integral parameters. Thus the data plotting, curve fitting, and slope measuring, which is the normal technique of obtaining experimental N values, is eliminated. The N values obtained by this method should be within the accuracy with which they could be measured.

Langley Research Center
National Aeronautics and Space Administration
Hampton, Virginia, August 20, 1974

REFERENCES

1. Tucker, Maurice: Approximate Turbulent Boundary-Layer Development In Plane Compressible Flow Along Thermally Insulated Surfaces With Application to Supersonic-Tunnel Contour Correction. NACA TN 2045, 1950.
2. Persh, Jerome; and Lee, Roland: Tabulation of Compressible Turbulent Boundary Layer Parameters. NAVORD Report 4282, Aeroballistics Report 337, U.S. Naval Ordnance Laboratory, White Oak, Maryland, May 1956 .
3. Monaghan, R.J.: An Approximate Solution of the Compressible Laminar Boundary Layer on a Flat Plate. ARC R&M No. 2760, 1949 .
4. Allen, Jerry M.: Evaluaiton of Compressible-Flow Preston Tube Calibrations. NASA TN D-7190, 1973.
5. Johnson, Charles.; and Bushnell, Dennis M.: Power-Law Velocity-Profile-Exponent Variations With Reynolds Number, Wall Cooling, and Mach Number in a Turbulent Boundary Layer. NASA TN D-5753, 1970 .

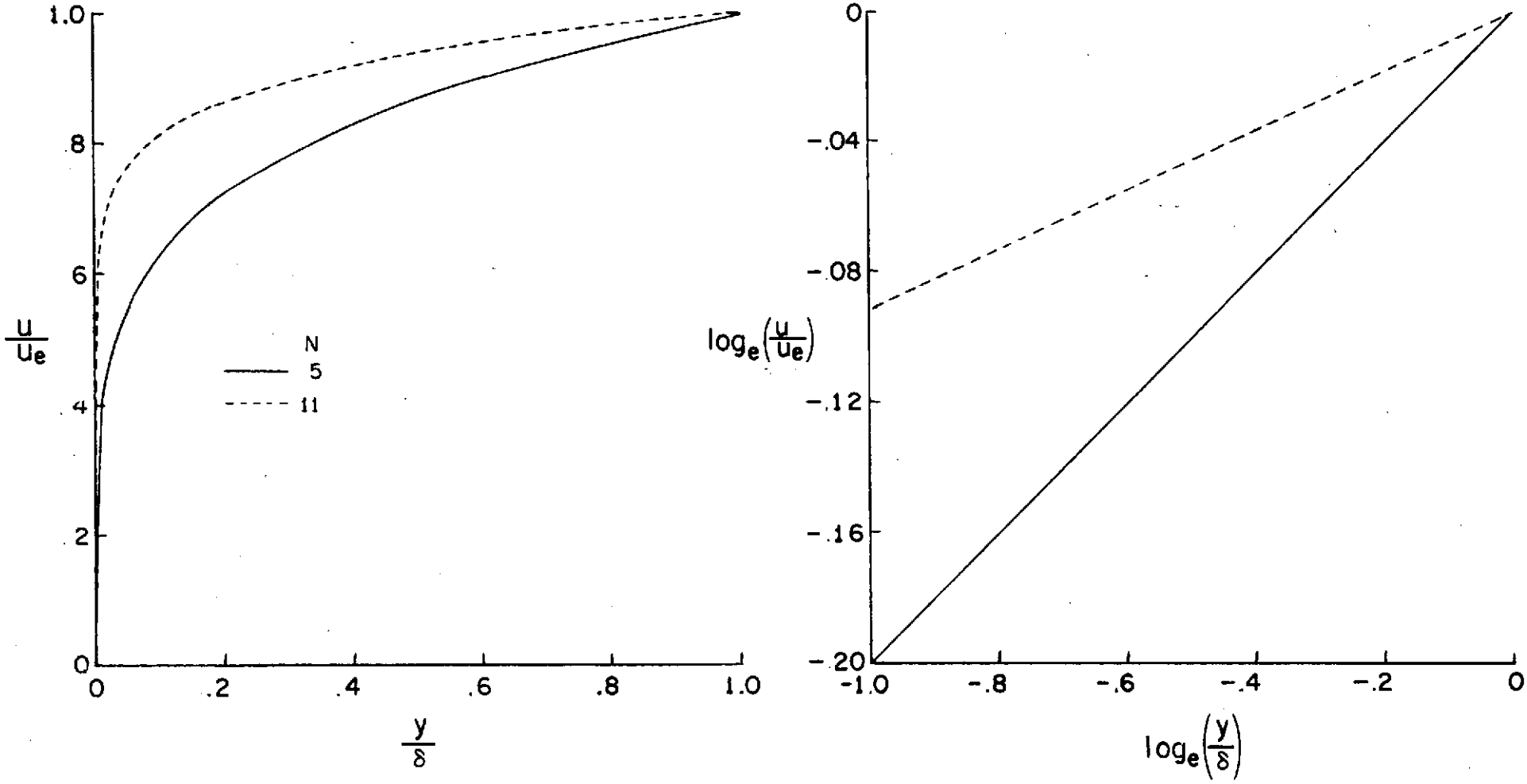

(a) Linear plot

(b) Logarithmic plot

Figure 1.- Boundary-Layer Power-Law Velocity Profiles

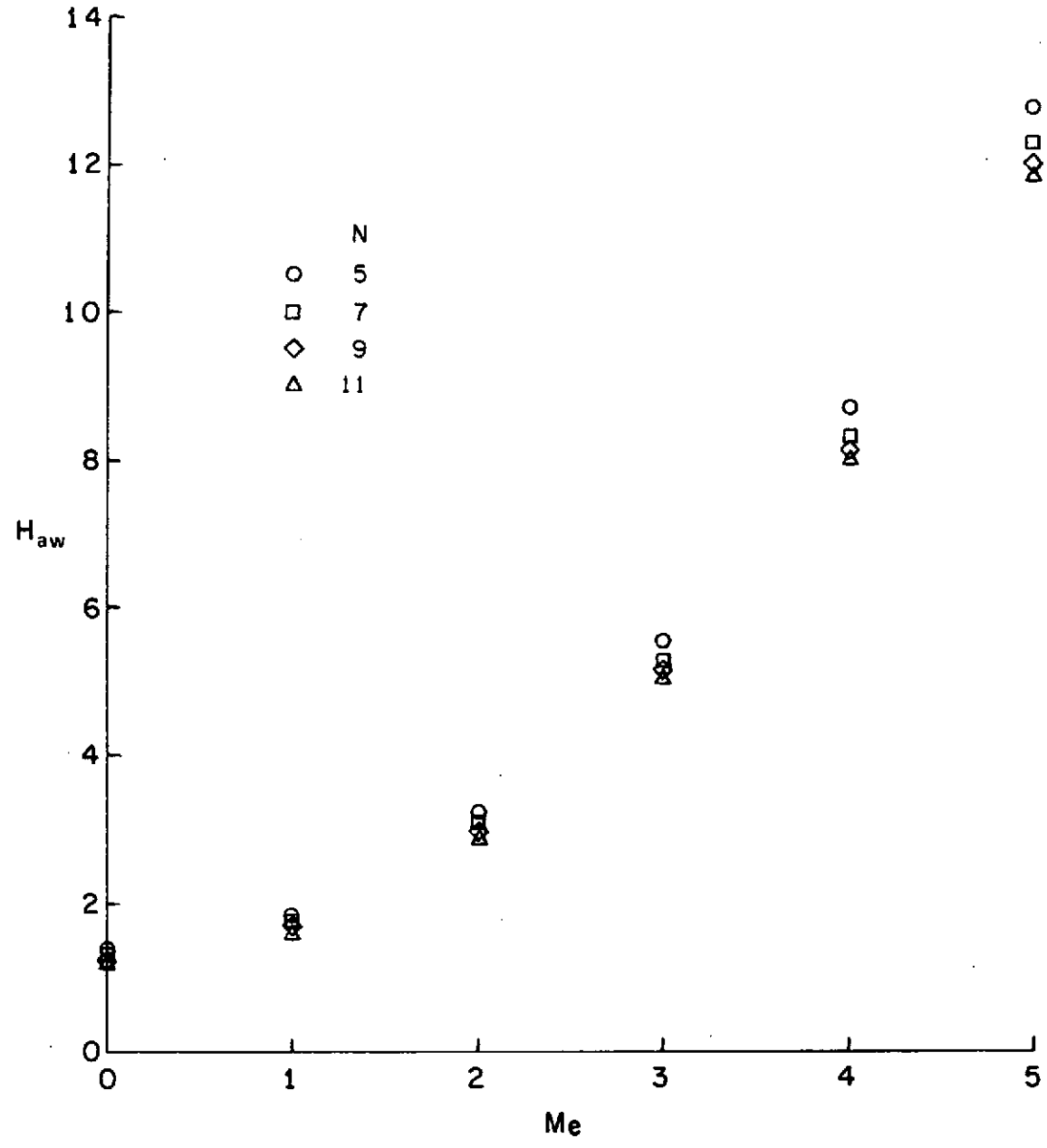

Figure 2.- Mach Number Effects on Adiabatic Turbulent Shape Factor

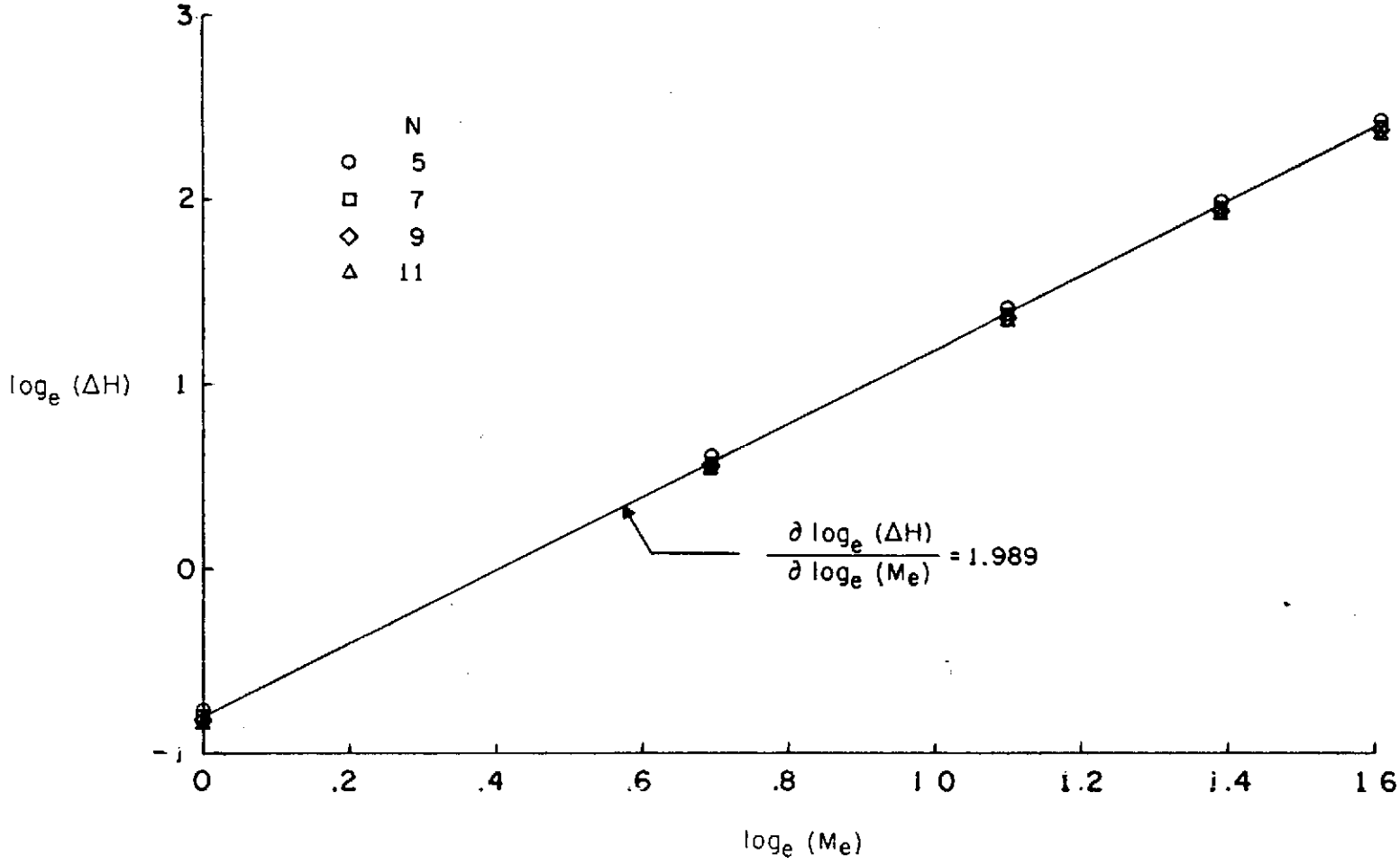

Figure 3.- Logarithmic Variation of ΔH with Mach Number

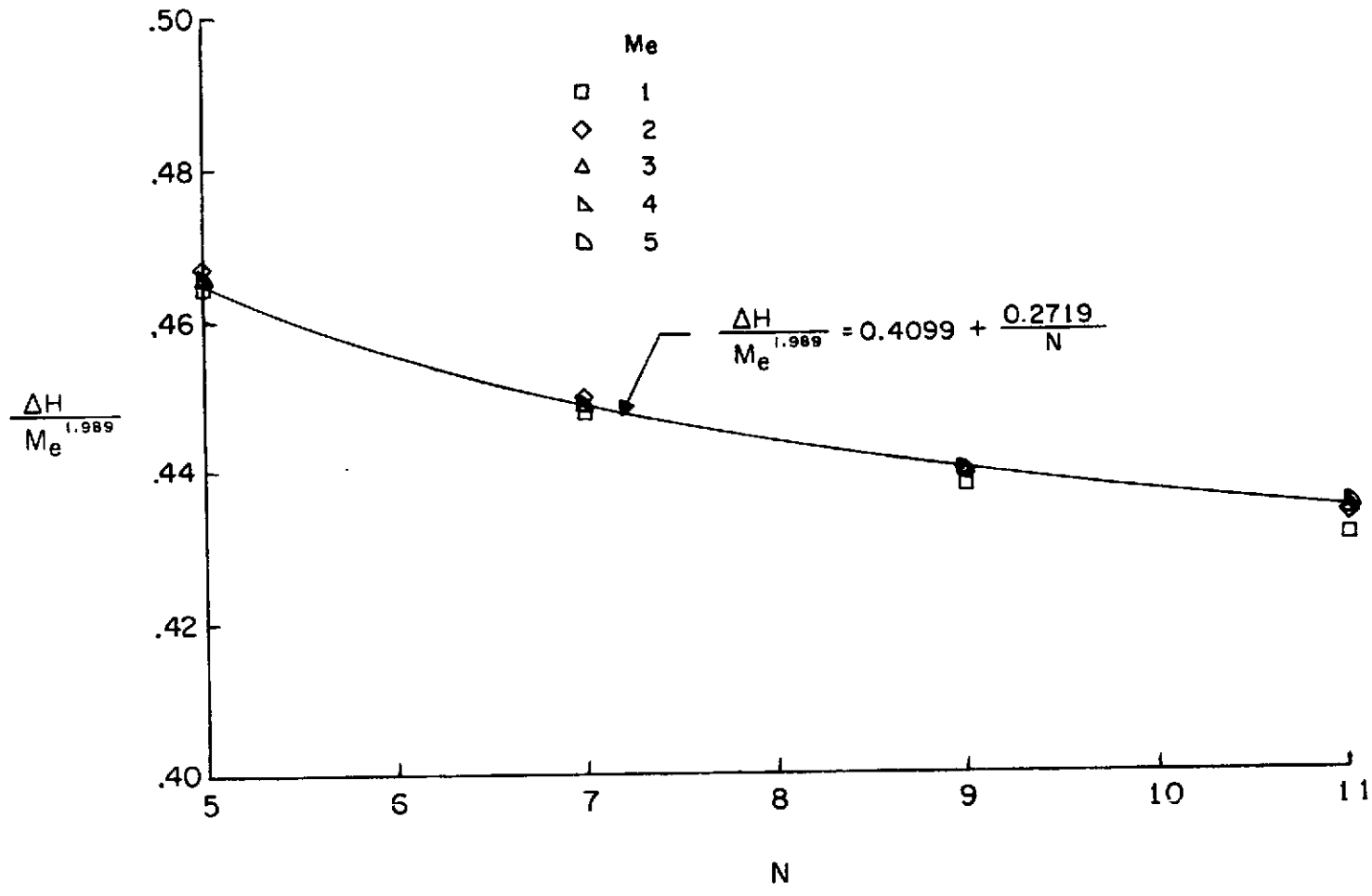

Figure 4.- Variation of Compressibility Parameter with Power-Law Exponent

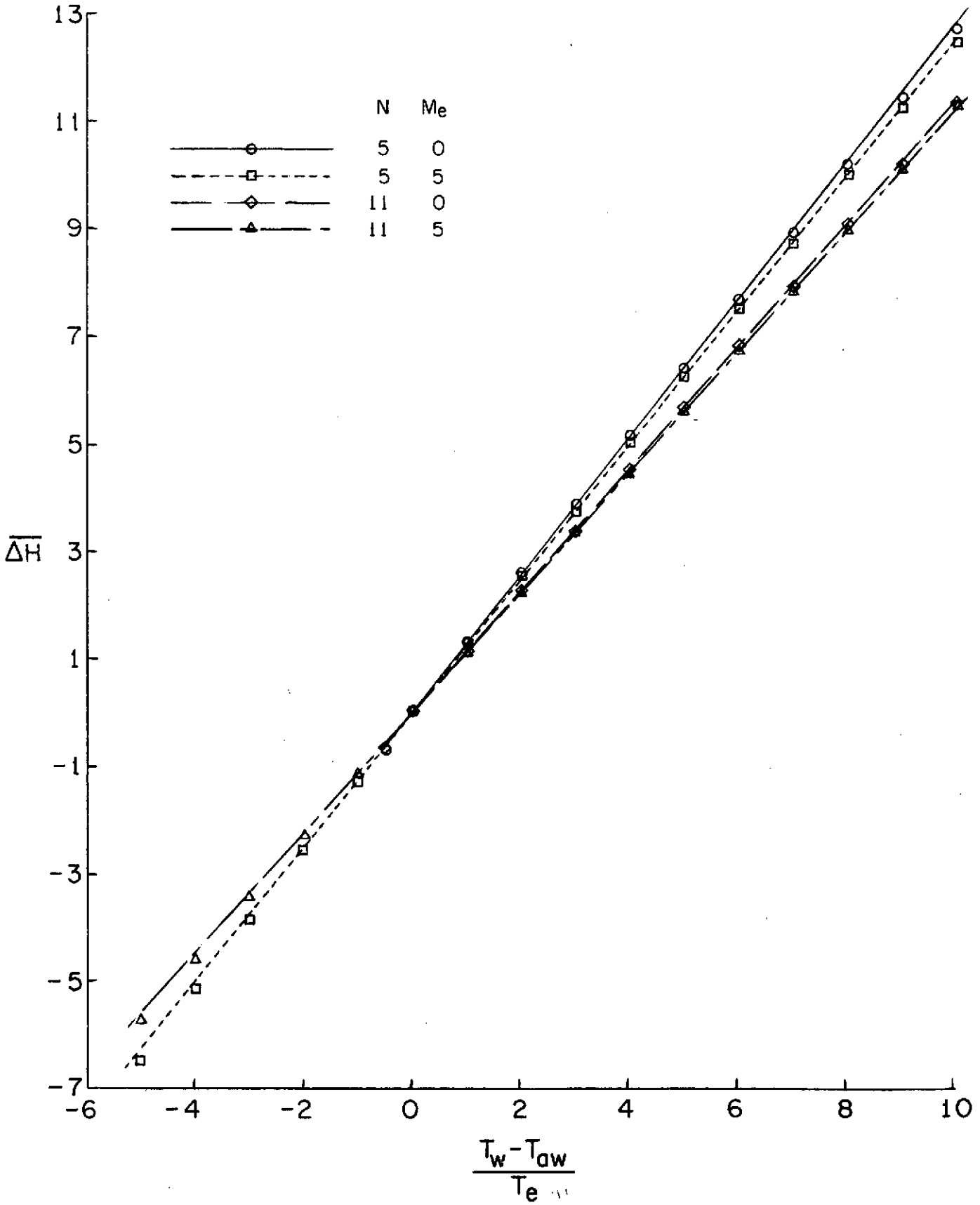

Figure 5. - Effect of Wall Temperature on Turbulent Shape Factor

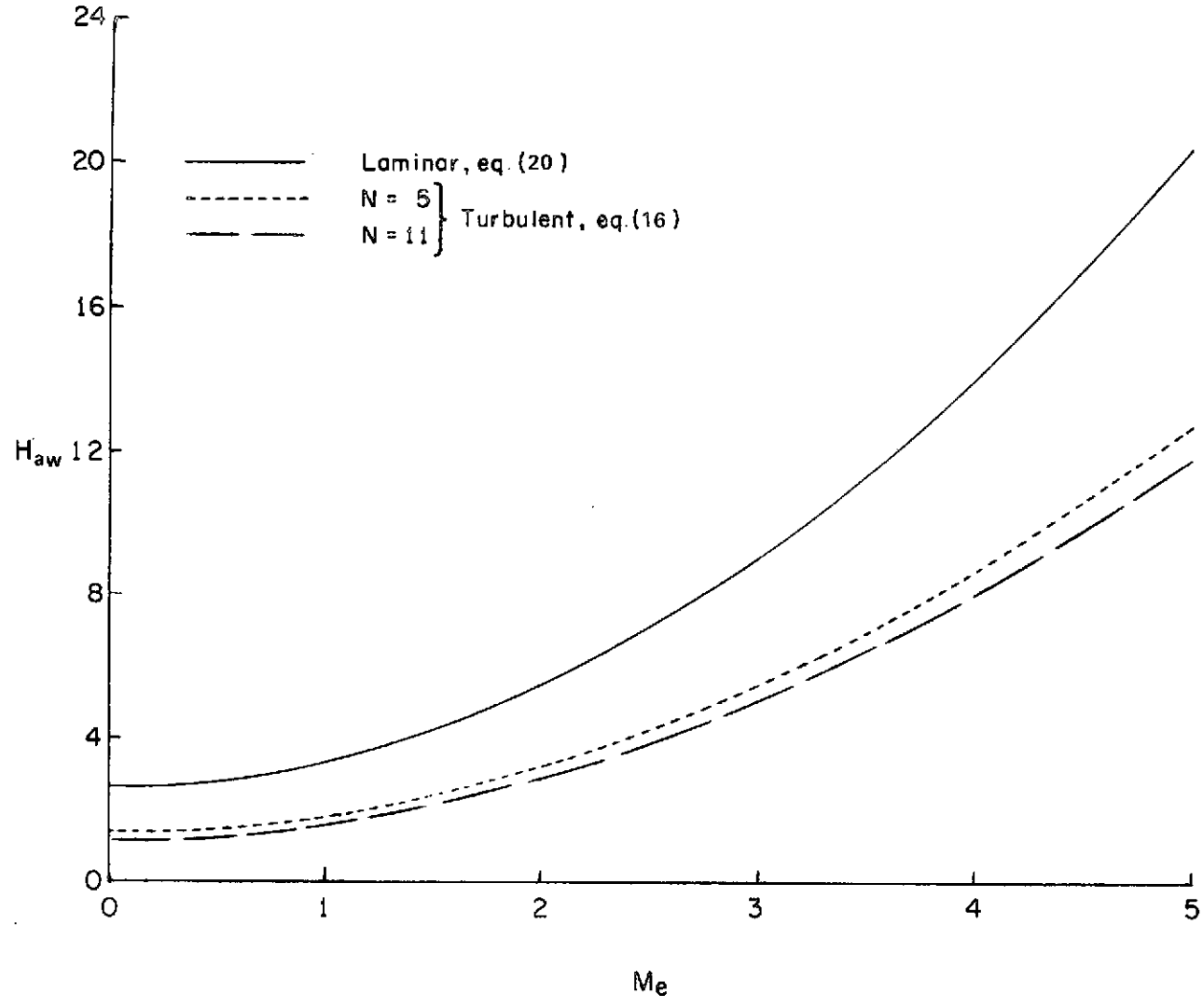

(a) Effect of Mach Number at $T_w = T_{aw}$

Figure 6. - Comparison of Laminar and Turbulent Shape Factors

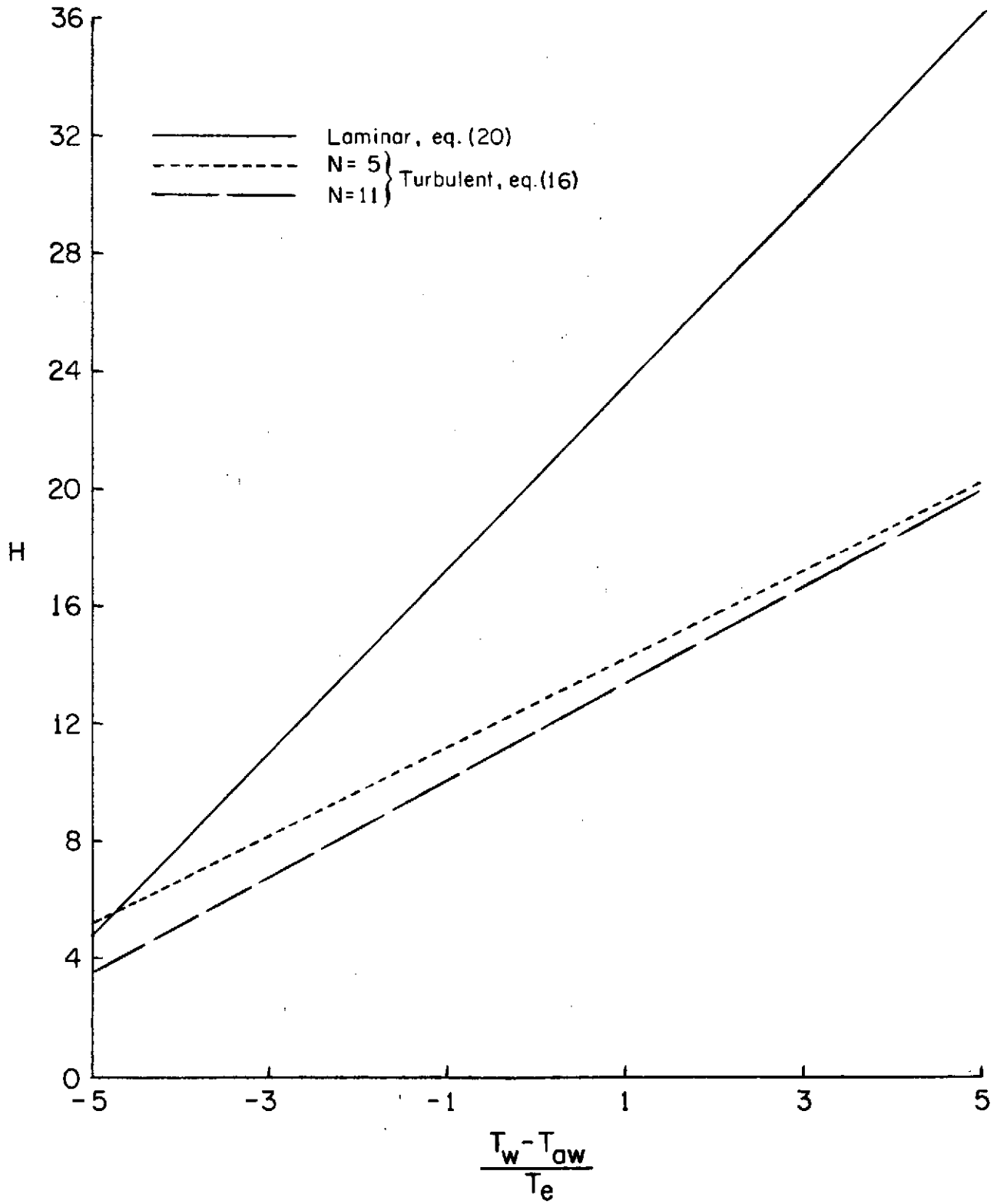

(b) Effect of Wall Temperature at $M_e = 5$

Figure 6.- Concluded

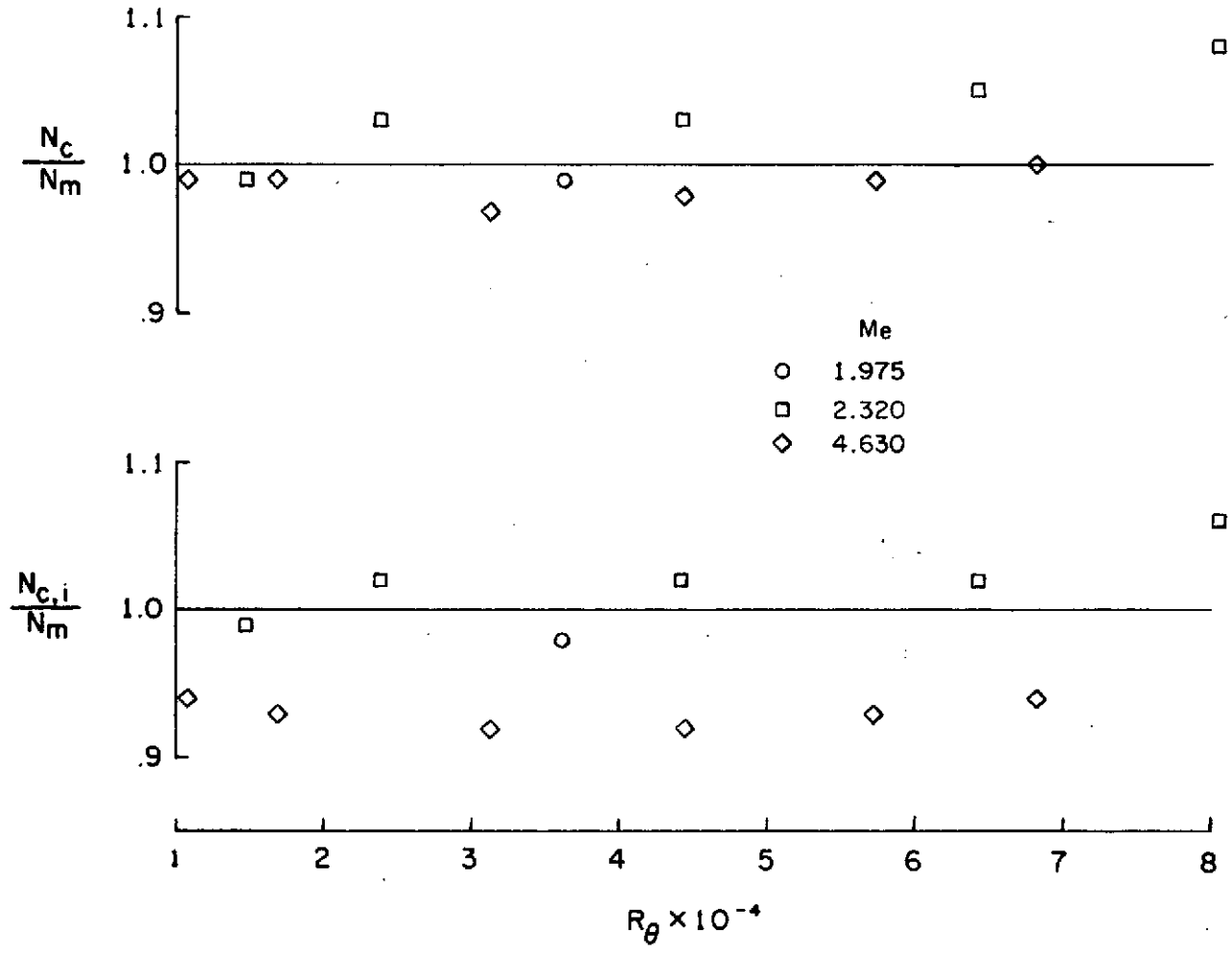

Figure 7.- Comparison of Calculated and Measured Power-Law Exponents

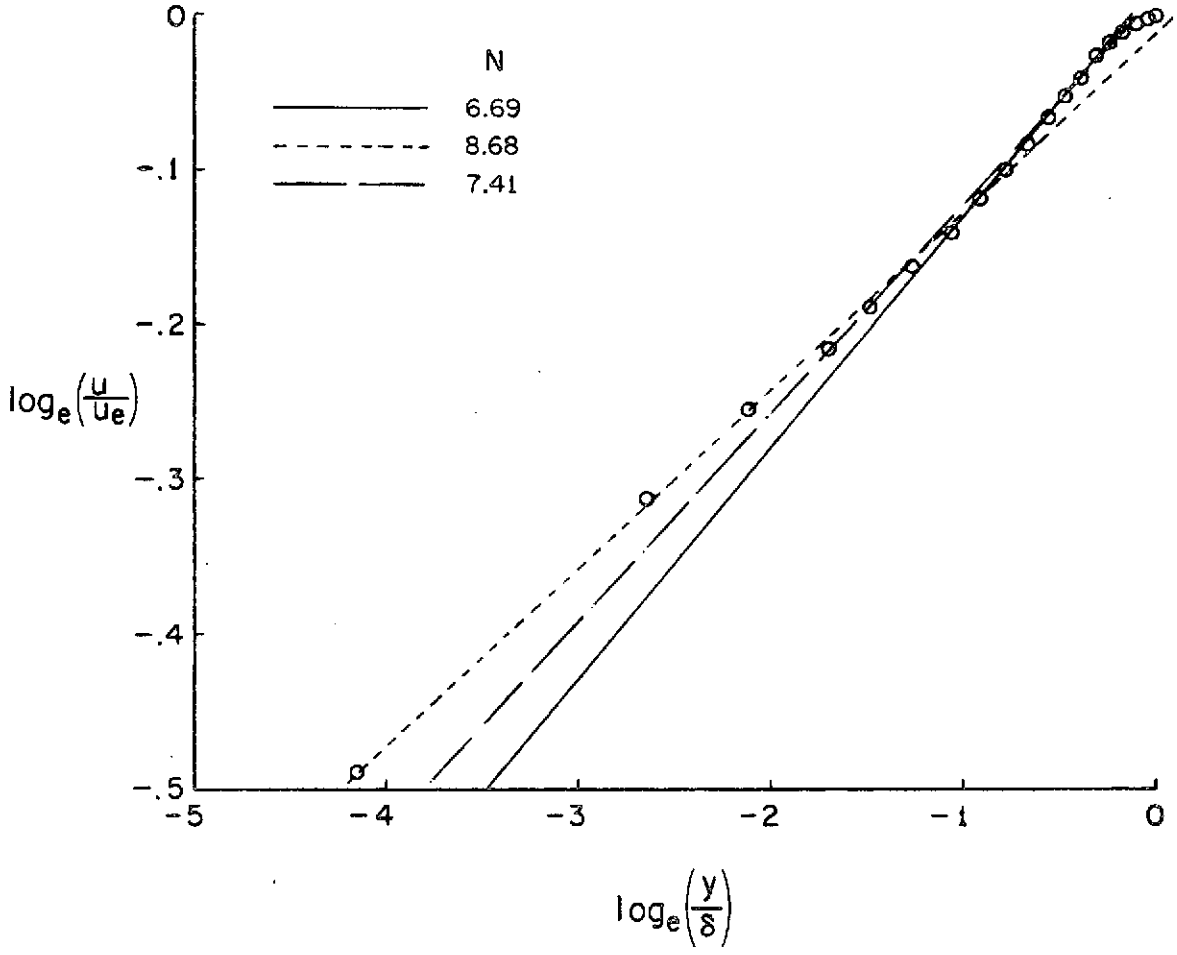

Figure 8.- Power-Law Curves Compared to Profile 1